TECHNICAL TRANSACTIONS | CZASOPISMO TECHNICZNE
CIVIL ENGINEERING | BUDOWNICTWO
2-B/2015

TOMASZ LIPECKI*

THE RELATIONSHIP BETWEEN WIND PRESSURE ON THE SURFACE OF RECTANGULAR PRISMS AND ATMOSPHERIC BOUNDARY LAYER PARAMETERS

ZALEŻNOŚĆ MIĘDZY CIŚNIENIEM WIATRU NA POWIERZCHNI OBIEKTÓW PROSTOPADŁOŚCIENNYCH A PARAMETRAMI WARSTWY PRZYŚCIENNEJ

Abstract

This paper considers the dependence of pressure fields on surfaces of rectangular prisms obtained from wind tunnel experiments on boundary layer characteristics. Six different variants of boundary layer flows were simulated in the wind tunnel. The qualitative coefficients of correlation R_s between the wind pressure coefficient C_p or its standard deviation σ_p and parameters describing boundary layer flows (wind speed profile, turbulence intensity profile, power spectral density) were estimated in order to determine how wind parameters influence surface pressure. Five rectangular prisms were placed in the wind tunnel. The following ratios of prism dimensions were adopted: $D/B/H$ = 1:2:20 (R5); 1:2:10 (R3); 1:2:5 (R1); 1:4:20 (R4); 1:4:10 (R2).

Keywords: wind action, wind tunnel, pressure coefficient, Spearman correlation coefficient

Streszczenie

W artykule przedstawiono analizę zależności ciśnienia zmierzonego na powierzchniach obiektów prostopadłościennych w trakcie badań wykonanych w tunelu aerodynamicznym od parametrów opisujących strukturę wiatru w warstwie przyściennej. W pomiarach przyjęto sześć różnych wariantów struktury wiatru. Wyznaczono jakościowy współczynnik korelacji R_s między współczynnikiem średniego ciśnienia C_p lub jego odchylenia standardowego σ_p na powierzchni modeli, a parametrami określającymi strukturę wiatru w warstwie przyściennej (pionowym profilem średniej prędkości wiatru, pionowym profilem intensywności turbulencji, funkcją gęstości widmowej mocy). Celem analiz było określenie wpływu poszczególnych parametrów wiatru na ciśnienie powierzchniowe. Pomiary wykonano na pięciu modelach prostopadłościanów o następujących stosunkach wymiarów: $D/B/H$ = 1:2:20 (R5), 1:2:10 (R3), 1:2:5 (R1), 1:4:20 (R4), 1:4:10 (R2).

Słowa kluczowe: oddziaływanie wiatru, tunel aerodynamiczny, współczynnik ciśnienia, współczynnik korelacji Spearmana

DOI: 10.4467/2353737XCT.15.127.4164

* Department of Structural Mechanics, Lublin University of Technology, Poland.

1. Introduction

Investigations of the pressure structure on the surfaces of prisms placed in the wind tunnel have been reported several times. The majority of experiments concerned 2D flows with constant wind speed and turbulence intensity and were related to square [1–5] and to rectangular cross-sections [4–7] mainly elongated along the mean wind speed. Some papers also refer to 3D flows, where prisms were placed vertically in the atmospheric boundary layer (ABL). Such measurements were mainly conducted on models with square cross-section [8–10] and seldom on rectangular cross-sections [11–13]. When 2D models and flows are taken into consideration, the determination of dependencies between surface pressure and wind parameters is rather simple. On the other hand, when prisms in the ABL are considered, the problem becomes more complicated. A detailed description of the ABL structure in the wind tunnel was reported in [14–28]. Generally, wind structure should be described by the following parameters: vertical profile of the wind speed v; vertical profile of the turbulence intensity I_v; length scale of turbulence L_v; power spectral density function of the wind speed (PSD). In more recent studies, the above parameters are related to three components of the wind speed vector (longitudinal, transverse and vertical).

There is an attempt to numerically describe the dependencies between surface pressure and several wind structure parameters in this paper. In order to investigate these dependencies, the qualitative coefficient of correlation (Spearman coefficient) R_s were calculated. Six different variants of the ABL structure were adopted in the wind tunnel simulations. Measurements of pressure were taken on the surfaces of five models with rectangular cross-sections. The ratio of the cross-section dimensions D/B was 2 for three models and 4 for two of them. The ratios of all dimensions were: $D/B/H$ = 1:2:20 (R5); 1:2:10 (R3); 1:2:5 (R1); 1:4:20 (R4); 1:4:10 (R2).

2. Description of wind tunnel measurements

All experiments were conducted in the boundary layer wind tunnel of Cracow University of Technology. Details of the wind tunnel specification and equipment can be found in [29].

Pressure on all faces of the rectangular prisms were measured during wind tunnel experiments. Different prisms of side ratio D/B = 1:2 (3 models) and D/B = 1:4 (2 models) were placed vertically on the rotational table in the measuring section of the wind tunnel. Dimensions of all models are presented in Table 1. Every prism was equipped with pressure taps at 16 levels along the height and around circumference (Fig. 1a). The angle of the wind attack was set at 15° increments from 0° to 90°. In the initial position (0°), the longer side of the prism was placed perpendicularly to the mean wind speed (Fig. 1b). The recorded dynamic pressure was averaged and normalized by the reference pressure measured at the front of the prism at a height of 70 cm. Detailed description of pressure measurements can be found in [30–32].

Six different cases of ABL flows were simulated in the wind tunnel. These correspond to consecutive terrain categories, and varied significantly in vertical profiles of the mean

wind speed, turbulence intensity, and power spectral density functions (PSD). A detailed description of ABL parameters is presented in [33]. Vertical profiles of the wind speed and turbulence are presented in Fig. 2.

Table 1

Geometric characteristics of prisms

Model	*H*	*B*	*D*	*H*/*D*	*B*/*D*
	[cm]	[cm]	[cm]	[-]	[-]
R1	100	40	20	5	2
R2	100	40	10	10	4
R3	100	20	10	10	2
R4	100	20	5	20	4
R5	100	10	5	20	2

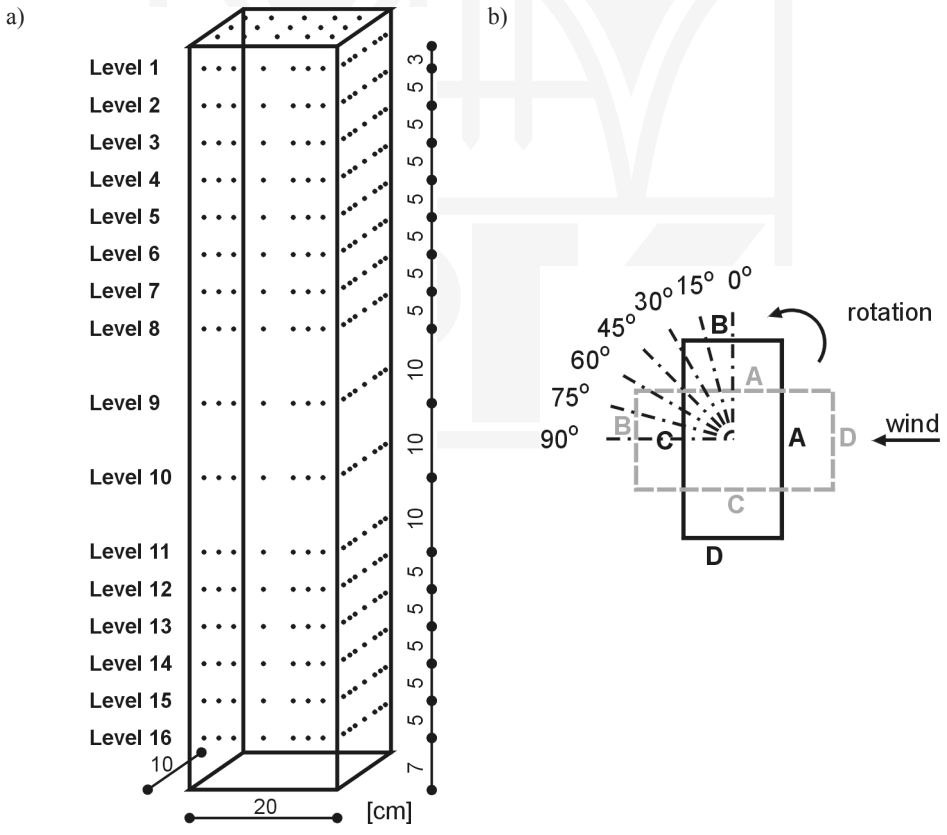

Fig. 1. a) Pressure taps locations on model R3, b) denotations of walls and angles of wind attack α_w

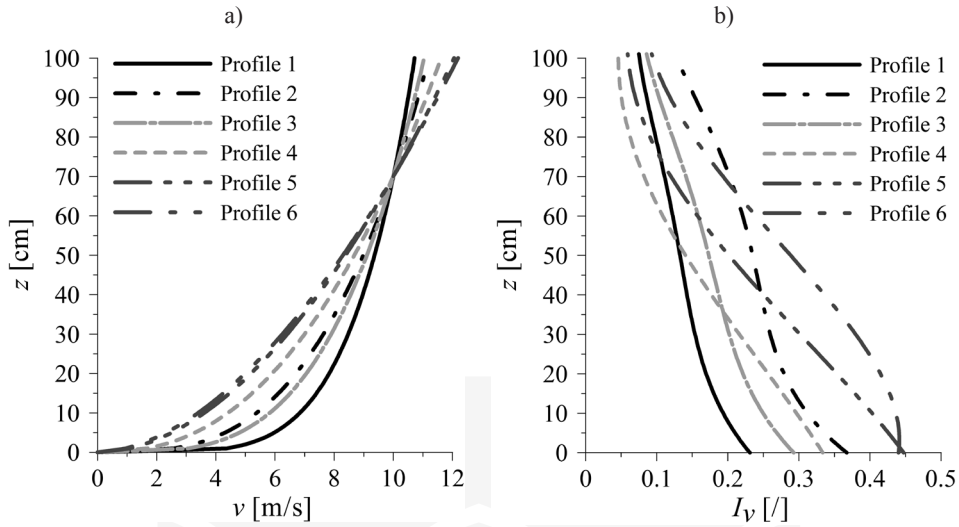

Fig. 2. a) Vertical profile of the mean wind speed v, b) vertical profile of turbulence intensity I_v

3. Spearman rank correlation

Qualitative correlation was calculated in order to estimate the dependence of surface pressure on ABL parameters. The Spearman rank correlation coefficient was chosen as a statistical instrument which allows the determination of such a relationship.

The coefficient describes qualitative dependence between wind structure parameters and pressure coefficients or its standard deviation. It can be used in cases where two variables are non-measurable and are of a qualitative nature, and their empirical values can be described by respective features of assumed ranks. Moreover, the data set has to be small. In the considered case, the data set is small, equal to 6 wind variants, and both wind parameters as well as pressure coefficients are treated as non-measurable values of respective ranks. Spearman coefficient can be calculated from the simple formula:

$$R_s = 1 - \frac{6\sum_{i=1}^{n} d_i^2}{n\left(n^2 - 1\right)} \tag{2}$$

where: n – number of probes, in that case is a number of wind structure variants, $n = 6$, d_i – difference between variables ranks.

Assignment of ranks is based on the consecutive numbering of features of two variables in ascending or descending sequence (from 1 to n). The limiting values for R_s are -1 and 1. $R_s = 0$ means independent variables, R_s in the range 0–0.3 means a lack of correlation, whereas in the range 0.9–1, a very strong correlation, finally $R_s = 1$ describes a full correlation between variables. Negative values can be interpreted in the same way.

In this paper, Spearman's coefficient was applied to investigate the dependence between the sequence of respective wind characteristics and the sequence of pressure coefficient C_p or its standard deviation σ_p on particular measurement levels. Wind structure variants were numbered from 1 to 6, according to Fig. 2. Every feature of the wind structure variants were then set from the highest value to the lowest on respective levels according to assumed numbers. To such segregated values, the appropriate ranks from 1 to 6 were applied. Rank 1 relates to the maximum value, rank 6 to the minimum value. Therefore, if the wind velocity on 97 cm for wind variant no 1 is the lowest then it will receive rank 6, whereas if the velocity for variant 6 is the highest, then it will receive rank 1 (Tables 2 and 3). Values of C_p or σ_p on the surfaces of particular walls and levels were arranged in the same way. For example, if C_p on 97 cm for the variant no. 2 of the wind structure is the highest, then it will receive a rank of 1, whereas on the same level, if C_p is minimum for variant no. 1, then the rank will be 6.

As dependent variables, the following features of wind structure simulated in the wind tunnel were assumed: 1) mean wind speed profile of longitudinal component, v; 2) turbulence intensity profile of longitudinal component of wind speed, I_v; 3) maximum of PSD function of longitudinal wind speed component, max *PSD*. Their correlations with dependent variables on the surfaces of prisms: 1) mean wind pressure coefficient C_p; 2) its standard deviation σ_p were calculated.

Due to the fact that in some cases the sequence of values of C_p and σ_p changed along the width of the wall at the same level, the average sequence was assumed.

Spearman's rank correlation coefficient R_s was calculated for all walls (A, B, C and D), at every measuring level (16 levels) and for all considered angles of wind attack (0°–90°), according to denotations presented in Fig. 1. Values above 0 indicate the consistency between the sequence of C_p or σ_p and respective wind characteristics. If R_s value is closer to 1 then consistency will be higher. This means that if respective wind characteristic values decrease, then respective values on the prism surface will also decrease. R_s below 0 mean that the decrease in wind characteristic values is connected to the increase of C_p or σ_p on the surfaces of models.

The example of the approach in single case (model R1, angle of wind attack 0°, measuring level 1, windward wall of the prism) is presented in Table 2, whereas ranks describing v, I_v. max *PSD* at particular heights are collected in Tables 3–5 (rank 1 – maximum value, rank 6 – minimum value). Ranks in Tables 3–5 are independent of the angle of wind attack and are related to wind parameters.

Table 2

Ranks of dependent variables, model R1, angle 0°, level 1 (97 cm), windward wall

Flow variant	$v(z)$	$I_v(z)$	Max *PSD*	C_p	σ_p
profile 1	6	4	5	6	5
profile 2	4	1	1	1	1
profile 3	5	3	3	4	3
profile 4	3	6	6	5	6
profile 5	2	5	4	3	4
profile 6	1	2	2	2	2

Table 3

Ranks of values of the mean wind speed, *v*, on respective measurement levels

H [cm]	97	92	87	82	77	72	67	62	52	42	32	27	22	17	12	7
profile 1	6	6	6	6	6	6	1	1	1	1	1	1	1	1	1	1
profile 2	4	4	4	4	4	4	3	3	3	3	3	3	3	3	3	3
profile 3	5	5	5	5	5	5	2	2	2	2	2	2	2	2	2	2
profile 4	3	3	3	3	3	3	4	4	4	4	4	4	4	4	4	4
profile 5	2	2	2	2	2	2	5	5	5	5	5	5	5	5	5	5
profile 6	1	1	1	1	1	1	6	6	6	6	6	6	6	6	6	6

Table 4

Ranks of values of the turbulence intensity, I_v, on respective measurement levels

H [cm]	97	92	87	82	77	72	67	62	52	42	32	27	22	17	12	7
profile 1	4	4	4	4	4	5	5	5	6	6	6	6	6	6	6	6
profile 2	1	1	1	1	1	1	1	2	2	2	3	3	3	3	3	3
profile 3	3	3	3	3	3	3	3	3	4	4	5	5	5	5	5	5
profile 4	6	6	6	6	6	6	6	6	5	5	4	4	4	4	4	4
profile 5	5	5	5	5	5	4	4	4	3	3	2	2	2	2	2	2
profile 6	2	2	2	2	2	2	2	1	1	1	1	1	1	1	1	1

Table 5

Ranks of values of the maximum of PSD function, *max* PSD, on respective measurement levels

H [cm]	97	92	87	82	77	72	67	62	52	42	32	27	22	17	12	7
profile 1	5	4	5	5	5	5	5	5	5	5	6	6	6	6	6	5
profile 2	1	1	1	1	1	1	1	2	2	2	3	4	2	1	1	1
profile 3	3	3	3	3	3	3	3	4	4	4	4	5	5	5	3	2
profile 4	6	6	6	6	6	6	6	6	6	6	5	3	4	4	5	6
profile 5	4	5	4	4	4	4	4	3	3	3	1	1	1	3	2	4
profile 6	2	2	2	2	2	2	2	1	1	1	2	2	3	2	4	3

4. Results and discussion

4.1. The relationship between pressure parameters and mean wind speed

Results which illustrate the correlation coefficient R_s between the order of C_p or σ_p values and the order of mean wind speed, v, values along the height of models are presented in

Figs 3–4, for two exemplary angles of wind attack $\alpha_w = 0°$ and $\alpha_w = 90°$, on consecutive walls of the prisms (A,B,C and D), and for all models (R1–R5).

On the windward wall (A, $\alpha_w = 0°–45°$ and D, $\alpha_w = 60°–90°$), R_s coefficient is above 0 (Fig. 3). Unexpectedly, the correlation is quite low with a maximum of about +0.6 on windward walls A and D on levels above 70 cm (at that height, the wind speeds in every ABL variant are equal). Values of R_s for different models are similar. Higher correlation is visible below 45 cm, but values differ significantly between models.

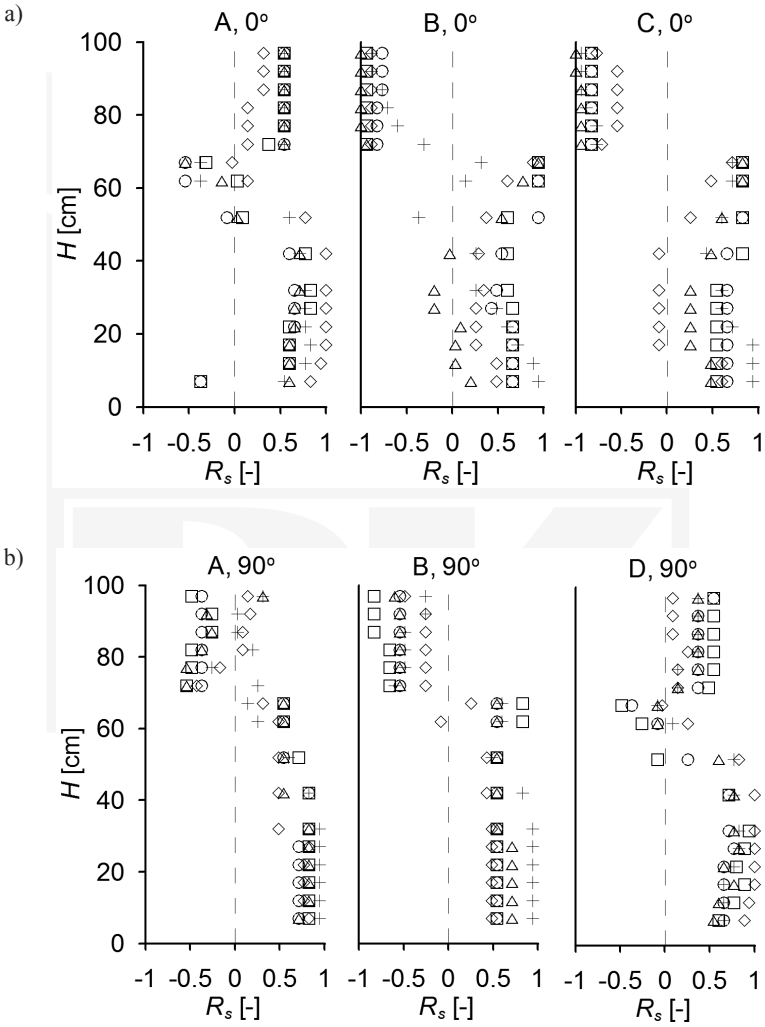

Fig. 3. Correlation coefficient R_s between the order of C_p and the order of the mean wind speed values: a) $\alpha_w = 0°$ A – windward wall, B (D – symmetric) – side wall, C – leeward wall; b) $\alpha_w = 90°$, A (C – symmetric) – side wall, B – leeward wall, D – windward wall, □ – model R1, ○ – model R2, ◇ – model R3, △ – model R4, + – model R5

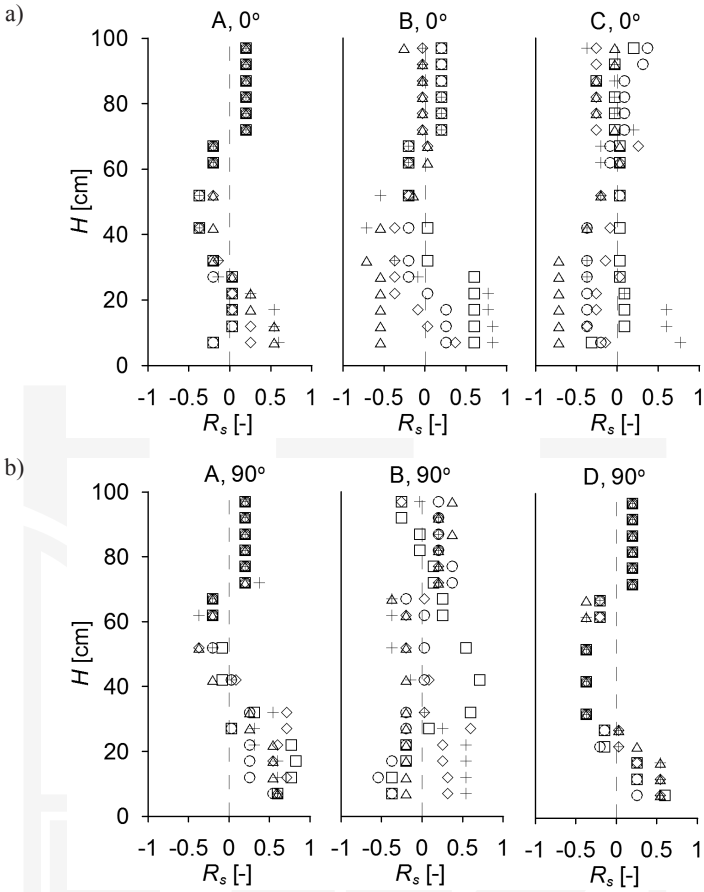

Fig. 4. Correlation coefficient R_s between the order of σ_p and the order of the mean wind speed values: a) $\alpha_w = 0°$; b) $\alpha_w = 90°$. Notations are as in Fig. 3

On side and leeward walls where the suction is, for all angles of wind attack, the values of R_s above 70 cm are close between models and are equal to a maximum of -1, so their correlation is very high (Fig. 3a – B, C and Fig. 3b – A, B). This means that when the speed increases (between ABL variants), the suction coefficient on walls will decrease (above 70 cm). For example, the wind speed in profile 6 is the highest at the top levels and this gives the lowest values of C_p on the leeward wall. Such a tendency to a lesser extent appears at $\alpha_w = 75°–90°$ for which R_s is lower and differences between models are high. Below a level of 70 cm, correlation coefficient changes its sign to +, and large discrepancies between models exist. Only for $\alpha_w = 90°$, the correlation coefficients are closer between models and their values approach +1. Positive values of R_s mean that when wind speed increases (between ABL variants) suction on walls will also increase (below 70 cm).

When considering the correlation between σ_p and wind speed, it can be noticed that R_s values are close to each other on walls with positive pressure, but correlation is very weak (about +0.2) on levels above 70 cm (Fig. 4a – A, Fig. 4b – D). On heights below that level,

the correlation coefficient changes its sign to '-', maximum to -0.5, and for heights around 30 cm again changes the sign to "+" and correlation slightly increases, maximum to +0.7, but the scatter of results between models also increases. On walls where the suction is, differences of R_s values between models are high. R_s values are lower above 70 cm and at that height, correlation is very weak or there is no correlation at all. Even a larger scatter of R_s appears below 70 cm, but values of R_s are higher and in the majority of cases, are negative, maximum to -0.7 (Fig. 4a – B, C, Fig. 4b – A, B)

4.2. The relationship between pressure parameters and turbulence intensity

Correlation coefficients R_s between pressure coefficient C_p or standard deviation σ_p and intensity of turbulence I_v, for $\alpha_w = 0°$ and $\alpha_w = 90°$ are presented in Figs 5–6.

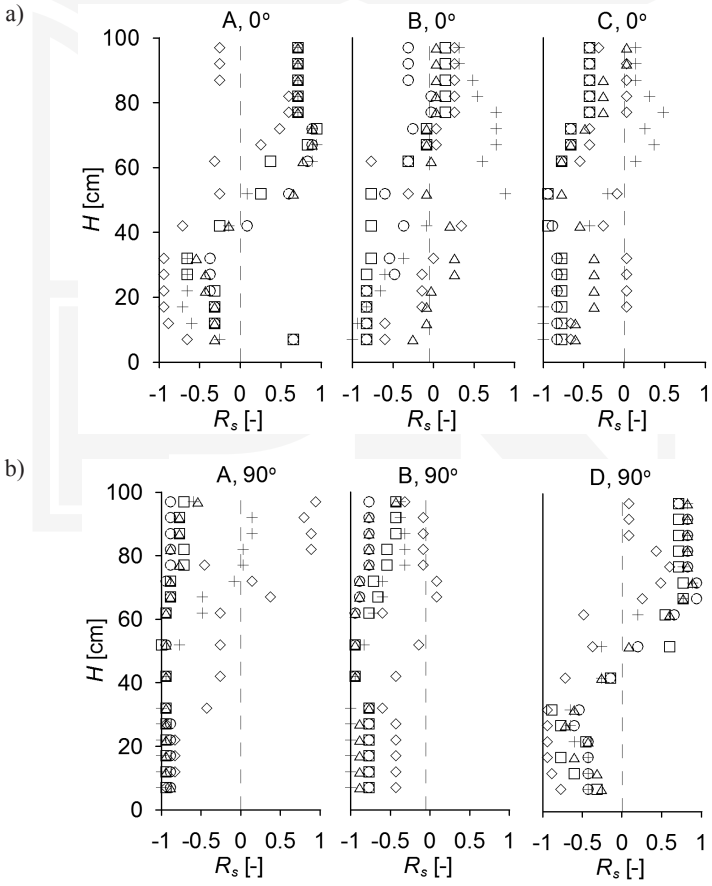

Fig. 5. Correlation coefficient R_s between the order of C_p and the order of the turbulence intensity values I_v. a) $\alpha_w = 0°$, b) $\alpha_w = 90°$. Notations are as in Fig. 3

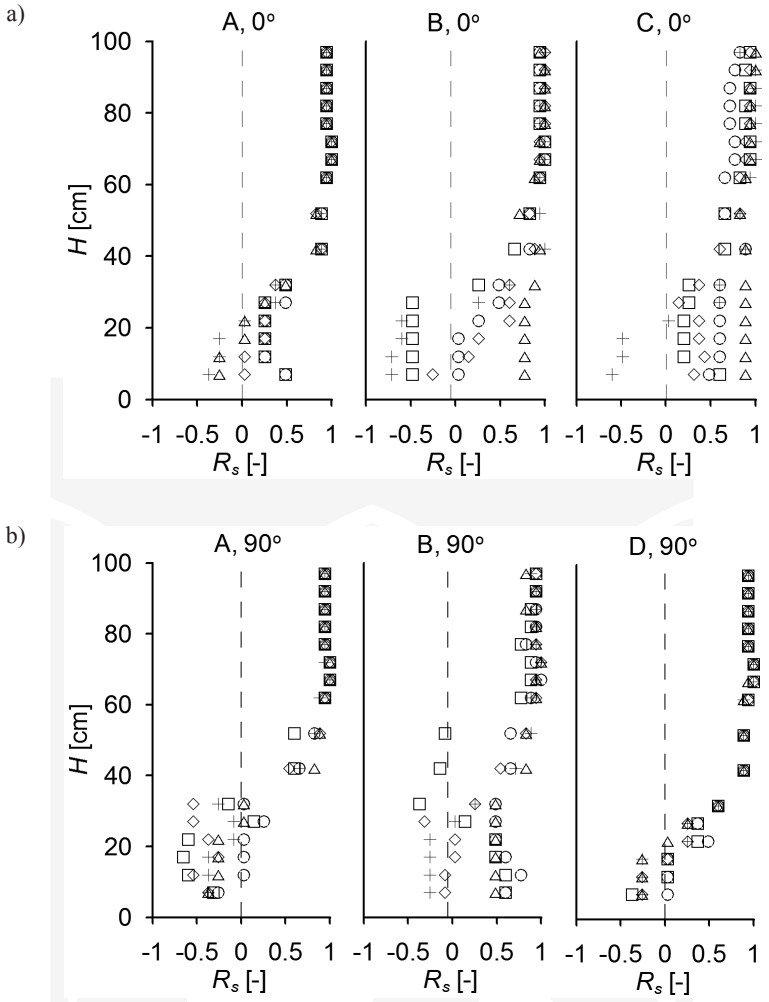

Fig. 6. Correlation coefficient R_s between the order of σ_p and the order or the turbulence intensity values I_v. a) $\alpha_w = 0°$, b) $\alpha_w = 90°$. Notations are like in Fig. 3

The correlation coefficient is positive, equal to +0.7–+0.8 above 70 cm on walls with positive pressure (Fig. 5a – A, Fig. 5b – D). Beneath 70 cm, the coefficient R_s is less than 0 and the scatter of results is larger, between -0.4 and -1. Correlation on walls with suction is low, with a different sign, and increases in direction to the support, where the sign is "-" (Fig. 5a – B, C). The scatter of results between models is considerable. For angles α_w = 75°–90° differences between models decrease and R_s is closer to -1 (Fig. 5b – A, B).

Coefficient R_s between σ_p and I_v above 40 cm is very high, close to +1 on every wall and for all angles of wind attack (Fig. 6a, b). Differences between models are negligible. Beneath 40 cm, correlation decreases and for angles $\alpha_w = 0°$ and α_w = 75°–90° achieves negative values with maximum of about -0.5 close to the support. The scatter of results is large.

4.3. The relationship between pressure parameters and maximum of PSD

Correlation coefficient R_s between C_p or σ_p and maximum of PSD function values (max *PSD*) for $\alpha_w = 0°$ and $\alpha_w = 90°$ are presented in Figs 7–8.

The R_s coefficient is positive, high or very high about +0.9 on walls with positive pressure above 70 cm (Fig. 7a – A, Fig. 7b – D). Differences between models are rather small. Beneath 70 cm, correlation decreases, changes sign, reaches a maximum of -0.9–-1 at 30 cm, then again changes sign and increases to about +0.9 at supports. When suction is on the walls, the negative correlation prevails on higher levels, but in some cases, also positive values appear (Fig. 7a – B, C, Fig. 7b – A, B). Generally, correlation is rather weak with maximum of about -0.7, with the exception of $\alpha_w = 75°–90°$ where it reaches -0.9. For all angles of wind attack, the highest correlation is at 40–50 cm and its maximum value is -1 ($\alpha_w = 75°–90°$). The R_s decreases in the direction to the base. There is considerable scatter between models for the whole height of all walls.

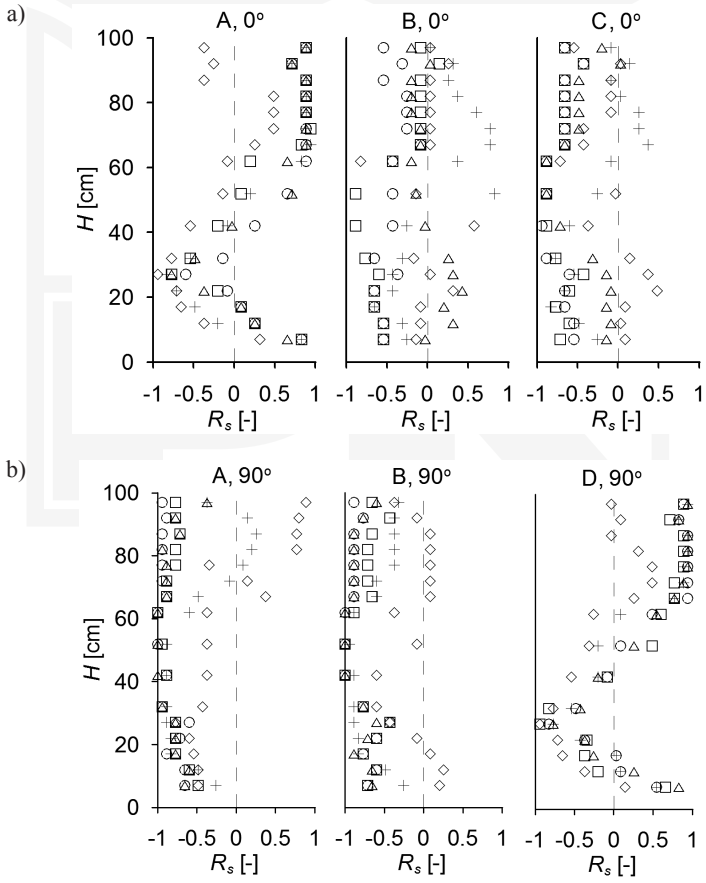

Fig. 7. Correlation coefficient R_s between the order of C_p and the order of the maximum values of PSD function, max *PSD*, a) $\alpha_w = 0°$, b) $\alpha_w = 90°$. Notations are as in Fig. 3

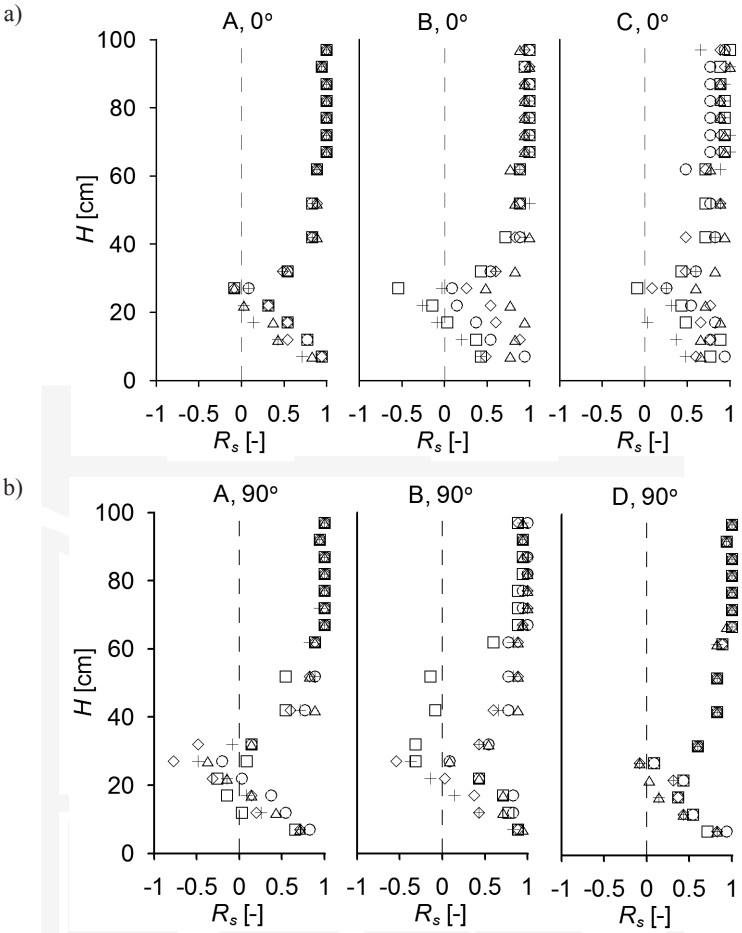

Fig. 8. Correlation coefficient R_s between the order of σ_p and the order of the maximum values of PSD function, max *PSD*, a) $\alpha_w = 0°$, b) $\alpha_w = 90°$. Notations are as in Fig. 3

A very high R_s, in the majority of cases equal to +1, is noticeable above about 60 cm when analyzing the correlation between max *PSD* and σ_p (Fig. 8a, b). Values between models are very close to each other. The coefficient decreases to a height of 25–30 cm where it is equal to 0 or changes sign. Below that height, R_s increases to 1 at the floor. The scatter of results also increases but is smaller on walls with positive pressure.

5. Conclusions

The attempt to numerically estimate the dependence between ABL parameters and rectangular prisms surface pressure parameters was undertaken in this paper. Two variables

of surface pressure were considered – the coefficient of the mean pressure C_p and its standard deviation σ_p. Three parameters of ABL were taken into account: vertical profile of the mean wind speed, v; turbulence intensity, I_v; the maximum value of PSD function, max *PSD*. Each group of parameters was treated as non-measurable values. The order of their values at respective levels was considered. The Spearman rank correlation coefficient was assumed and calculated as a measure which allows describing that dependence. In general, surprisingly, it seems that the higher correlation is between σ_p and flow characteristics than between C_p and respective flow characteristics. A more clear dependence is for σ_p. When considering the correlation between C_p and wind parameters, the scatter of results along the height is considerable. In the upper parts of the models, closer to their free ends, correlation coefficients are higher and generally better ordered; moreover, the values are closer to each other than at bottom levels.

References

[1] Vickery B.J., *Fluctuating lift and drag on a long cylinder of square cross-section in a smooth and in a turbulent stream*, Journal of Fluid Mechanics, Vol. 25(3), 1966, 481-491.

[2] Saathoff P., Melbourne W.H., *Effects of free stream turbulence on streamwise pressure measured on a square-section cylinder*, Journal of Wind Engineering and Industrial Aerodynamics, Vol. 79, 1999, 61-78.

[3] Lee B.E., *The effect of turbulence on the surface pressure field of a square prism*, Journal of Fluid Mechanics, Vol. 69(2), 1975, 263-282.

[4] Miyata T., Miyazaki M., *Turbulence effects on aerodynamic response of rectangular bluff cylinders,* Cermak J.E. (Ed.), *Wind Engineering*, Proc. 5th International Conference on Wind Engineering, Fort Collins, Colorado, USA, July 1979, 631-642.

[5] Noda H., Nakayama A., *Free-stream turbulence effects on the instantaneous pressure and forces on cylinders of rectangular cross section*, Experiments in Fluids, Vol. 34, 2003, 332-344.

[6] Li Q.S., Melbourne W.H., *Effects of turbulence on surface pressures of the flat plate and rectangular cylinders in separated and reattaching flows*, Proc. 9th International Conference on Wind Engineering, New Delhi, India, 1995, 165-176.

[7] Li Q.S., Melbourne W.H., *The effects of large scale turbulence on pressure fluctuations in separated and reattaching flows*, Journal of Wind Engineering and Industrial Aerodynamics, Vol. 83, 1999, 159-169.

[8] Kareem A., Cermak J.E., *Pressure fluctuations on a square building model in boundary-layer flows,* Journal of Wind Engineering and Industrial Aerodynamics, Vol. 16, 1984, 17-41.

[9] Sitheeq M.M., Iyengar A.K.S., Farell C., *Effect of turbulence and its scales on the pressure field on the surface of a three-dimensional square prism*, Journal of Wind Engineering and Industrial Aerodynamics, Vol. 69-71, 1997, 461-47l.

[10] Butler K., Cao S., Kareem A., Tamura Y., Ozono S., *Surface pressure and wind load characteristics on prisms immersed in a simulated transient gust front flow field*, Journal of Wind Engineering and Industrial Aerodynamics, Vol. 98, 2010, 299-316.

[11] Kareem A., *Measurements of pressure and force fields on building models in simulated atmospheric flows*, Journal of Wind Engineering and Industrial Aerodynamics, Vol. 36, 1990, 589-599.
[12] Cheng C.M., Tsai M.S., *Along wind design wind load for tall buildings (I) Results of wind tunnel tests*, Proc. 5th International Advanced School on wind Engineering, The GCOE Program at Tokyo Polytechnic University, Poland, Opole 2009.
[13] Rosa L., Tomasini G., Zasso A., Aly A.M., *Wind-induced dynamics and loads in a prismatic slender building: A modal approach based on unsteady pressure measurements*, Journal of Wind Engineering and Industrial Aerodynamics, Vol. 107-108, 2012, 118-130.
[14] Counihan J., *Simulation of an adiabatic urban boundary layer in the wind tunnel*, Atmospheric Environment, Vol. 7, 1973, 673-689.
[15] Robins A.G., *The development and structure of simulated neutrally stable atmospheric boundary layers*, Journal of Wind Engineering and Industrial Aerodynamics, Vol. 4, 1979, 71-100.
[16] Farell C., Iyengar A.K.S., *Experiments on the wind tunnel simulation of atmospheric boundary layers*, Journal of Wind Engineering and Industrial Aerodynamics, Vol. 79, 1999, 11-35.
[17] Witter A.R., Möller S.V., *Characteristics of the low-speed wind tunnel of the UNNE*, Journal of Wind Engineering and Industrial Aerodynamics, Vol. 84, 2000, 307-320.
[18] Iyengar A.K.S., Farell C., *Experimental issues in atmospheric boundary layer simulations: roughness length and integral length scale determination*, Journal of Wind Engineering and Industrial Aerodynamics, Vol. 89, 2001, 1059-1080.
[19] Balendra, T., Shah, D.A., Tey, K.L., Kong, S.K., *Evaluation of flow characteristics in the NUS-HDB Wind Tunnel*, Journal of Wind Engineering and Industrial Aerodynamics, Vol. 90, 2002, 675-688.
[20] De Bortoli M.E., Natalini B., Paluch M.J., Natalini M.B., *Part-depth wind tunnel simulations of the atmospheric boundary layer*, Journal of Wind Engineering and Industrial Aerodynamics, Vol. 90, 2002, 281-291.
[21] Chen K., Jin X.Y., Zhao J.D., *Design and characteristics of a large boundary layer wind tunnel with two test sections*, Proc. 7th Asia-Pacific Conference on Wind Engineering, Taipei, Taiwan, 2009, CD.
[22] Kozmar H., *Scale effects in wind tunnel modeling of an urban atmospheric boundary layer*, Theoretical and Applied Climatology, Vol. 100(1-2), 2010, 153-162.
[23] Kozmar H., *An alternative approach to experimental simulation of wind characteristics in urban environments*, Procedia Environmental Sciences, Vol. 4, 2011, 43-50.
[24] Kozmar H., *Truncated vortex generators for part-depth wind-tunnel simulations of the atmospheric boundary layer flow*, Journal of Wind Engineering and Industrial Aerodynamics, Vol. 99, 2011, 130-136.
[25] Kozmar H., *Characteristics of natural wind simulations in the TUM boundary layer wind tunnel*, Theoretical and Applied Climatology, Vol. 106, 2011, 95-104.
[26] Kozmar H., *Physical modeling of complex airflows developing above rural terrains*, Environmental Fluid Mechanics, Vol. 12, 2012, 209-225.
[27] Varshney K., Poddar K., *Experiments on integral length scale control in atmospheric boundary layer wind tunnel*, Theoretical and Applied Climatology, Vol. 106, 2011, 127-137.

[28] Varshney K., *Tailoring wind properties by various passive roughness elements in a boundary-layer wind tunnel*, International Journal of Physical Sciences, Vol. 7(8), 2012, 1182-1186.
[29] Flaga A. Lipecki T. (eds.), *Environmental effects on buildings, structures, materials and people*, Lublin 2007.
[30] Lipecki T., Bęc J., Błazik-Borowa E., *Surface pressures on rectangular cylinders – the dependence on aspect ratio, wind structure and angle of wind attack*, Proc. 7th Symposium on Bluff Body Aerodynamics and Applications, China, Shanghai 2012.
[31] Lipecki T., Jamińska P., *Analysis of wind pressure distribution on the surface of 2:1 rectangular cylinder*, Proc. XX Fluid Mechanics Conference, Poland, Gliwice 2012.
[32] Lipecki T., *Oddziaływanie wiatru na budynki wysokie w świetle badań własnych i ujęć normowych*, Budownictwo i Architektura, Vol. 12(2), 2013, 143-150.
[33] Bęc J., Lipecki T, Błazik-Borowa E., *Research on wind structure in the wind tunnel of Wind Engineering Laboratory of Cracow University of Technology*, Journal of Physics: Conference Series 318, 072003, doi: 10.1088/1742-6596/318/7/072003, 2011.